Elastic waveform inversion for rock property estimation and for imaging: A Midland Basin case study

Anthony Vassiliou, GeoEnergy Inc.; Rodney Stromberg, Lionel Woog, GeoEnergy Inc.*

Summary

Elastic waveform inversion (EWI) was employed in a Midland Basin 3-D survey with two objectives. The first objective was to estimate rock properties for developing unconventional reservoirs. Rock property volumes are used to map carbonate debris flows, define ductile and brittle zones, define facies and build geological models for the field. The second objective was to investigate improved imaging through the use of the EWI based compressional wave reflectivity as compared to the production prestack time migrated stack. By accurately estimating elastic parameters, we are able to compute rock properties necessary for the field development. The combination of improved imaging through post-migration EWI and accurate rock property imaging allows substantially better mapping of the Wolfcamp and Spraberry formations and can lead to potentially better well placement when combined with fracture detection and microseismic.

Introduction

For the purpose of developing unconventional reservoirs, the combination of high quality imaging and accurate rock property estimation is essential. Typically, prestack time/depth imaging coupled with simultaneous seismic inversion is used for seismic mapping, seismic stratigraphy and geological model development. In the present study, we compared EWI together with simultaneous seismic inversion (Hampson et al, 2005). In addition, we computed the EWI based P-wave reflectivity, and we compared it to the prestack time migration stack. Elastic waveform inversion theory was developed in the late 1990s and early 2000s (Roy, et al., 2004). Elastic waveform case studies have been reported before in Lau, et al. (2007) and Hilliard, Vassiliou (2010).

In this case study, we present a blind first application of post-migration EWI to an unconventional producing reservoir in the Midland Basin, using only one well for inversion parameterization. We show that the post-migration EWI results are superior to the simultaneous seismic inversion results and yield accurate rock property blind estimates. Furthermore, we demonstrate that the post-migration EWI generates a P-wave reflectivity imaging result that is substantially better than the conventional prestack time imaging stack.

Method

The shallow geology in the Permian Basin comprises Quaternary alluvial and aeolian deposits overlying the high velocity Cretaceous Edwards Limestone. Below the limestone are low velocity Cretaceous Trinity sands and Triassic Copper Canyon, Trujillo, and Tecova sands and shales and the Santa Rosa Sandstone followed by Permian anhydrites and dolomites in the Grayburg and San Andres formations. The deeper targets for unconventional reservoir development are the Spraberry and multiple Wolfcamp formations.

The land 3-D seismic data used in this study is a subset of a larger survey and includes 20559 Vibroseis shots and 9300 channels. The 3-D seismic data acquisition was wide azimuth and had maximum offsets of 60,000 ft. The seismic bandwidth was 3-95 Hz and the CDP bin spacing was 82.5 ft. The raw field shot gathers were first geometry checked and a spherical divergence correction was applied with a picked brute velocity. The first arrival traveltimes were then picked on the data set and subsequently inverted with a non-linear tomography from topography. The tomography traveltime RMS error was 8.5 ms. After the traveltime tomography, tomostatics were applied, and then the following processing steps were applied: a) minimum phase conversion, b) CMP gather denoising, c) surface consistent deconvolution with 180 ms operator and 24 ms gap, d) three passes of velocity analysis at 0.5 x 0.5 mile spacing, e) a proprietary seismic scaling, f) three passes of residual reflection statics and finally g) migration velocity scanning for migration velocity analysis. The prestack time migration residual moveout correction was then applied.

The resulting time imaging result was of high quality and correlated the well log synthetic seismogram used in this study with a 0.78 correlation coefficient.

The EWI case study was conducted on a 10 square mile subset area of a 3-D survey. The inputs to both the EWI and the simultaneous seismic inversion were the prestack time migrated gathers, the picked seismic horizons and one of the four wells available in this area. The three remaining wells were used as blind wells for the seismic inversion test.

The post-migration EWI uses the prestack time migrated gathers after NMO correction removal and a Ricker wavelet with peak frequency of 40 Hz. For the purpose of direct comparison of the EWI with the simultaneous seismic inversion results, we also generated a set of strictly flattened gathers. Therefore, the EWI uses two sets of prestack time migrated gathers, one with only residual moveout correction applied and with strict gather flattening applied to it. The simultaneous seismic inversion uses the gathers with the strict gather flattening applied, and subdivided into 15 angle stacks.

The results from the comparison of the EWI vs the simultaneous seismic inversion on the well farthest away from the well used in the inversion are shown in Figures 1a 1b, 1c, and 1d for the P-wave velocity estimation, 2a and 2b for the S-wave velocity estimation and 3a and 3b for the bulk density estimation. From these figures, it is clear that the EWI matches the blind well log better than the simultaneous seismic inversion. Also, overall the elastic waveform inversion using only residual move-out correction and non-strict flattened gathers yields better results than when the strict flattened gathers are used. Simultaneous seismic inversion works requires that the input gathers be conditioned at very flat. The forced flattening of the gathers can sometimes change small kinematics in the wavefield that are necessary for a proper inversion.

The Spraberry formation is a fairly low reflectivity formation, and it is difficult to map on the prestack time migration stack. The EWI was able to image this low reflectivity formation to a reasonable extent as shown in figures 1a and 1b compared to the full stack. Also within the Wolfcamp formation, the thin carbonate debris flow is better resolved and more continuous at 1325 ms, close to the blind well, in the EWI result than in the simultaneous inversion. The EWI was also able to better resolve the lower Wolfcamp C reflection event at 1500 ms. The bulk density EWI inversion also resolves the Spraberry Wolfcamp formations better in Figure 3a. Neither the simultaneous inversion or the EWI density results correlate very well with the bandpass filtered blind well log as shown in Figure 3b. The band pass filtered bulk density may not be adequate for the seismic inversion comparison. A larger area with more wells would be needed for a better comparison.

The EWI P-wave section provided higher resolution and better lateral continuity of reflections in the Spraberry and Wolfcamp sections than the time migration stack. To map these reflections we computed the P-wave reflectivity from the elastic waveform inversion results, and compared it to the standard prestack time imaging stack as shown in Figure 4. The elastic waveform inversion derived P-wave reflectivity has wider seismic bandwidth and also better spatial resolution than the prestack time imaging stack. Lateral wells can be positioned more accurately on the EWI reflectivity section in both the Spraberry and Wolfcamp sections. Faults are also better imaged in the EWI reflectivity than in the full stack.

Conclusion

Post-migration prestack elastic waveform inversion yields accurate P-wave velocity and S-wave velocity inversion, P-wave impedance and S-wave impedance results for rock property estimation than simultaneous inversion. In addition, EWI results yield a P-wave reflectivity volume with wider seismic bandwidth and higher spatial resolution than the conventional PSTM stack, leading to a seismic interpretation with a higher degree of confidence.

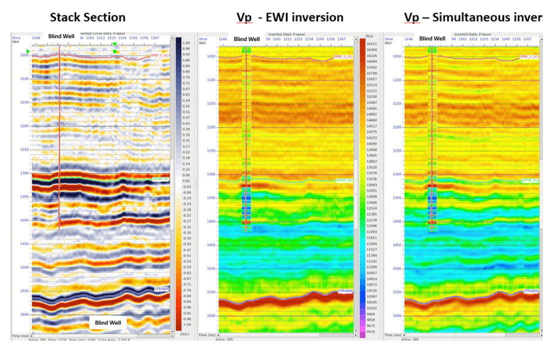

Figure 1a: Vp velocity comparison of EWI with strict flattened gathers (center) vs. simultaneous prestack seismic inversion (right)

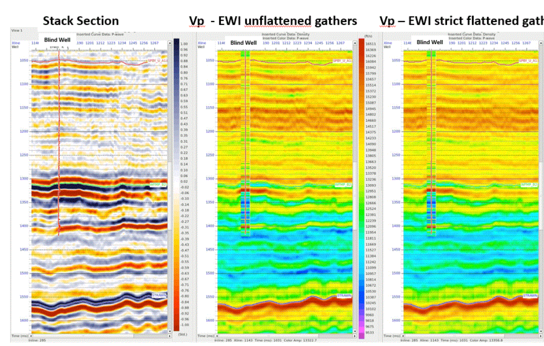

Figure 1b: Comparison of EWI with non strict flattened gathers (center) vs. strict flattened gathers (right).

Elastic waveform inversion for rock property estimation and for imaging

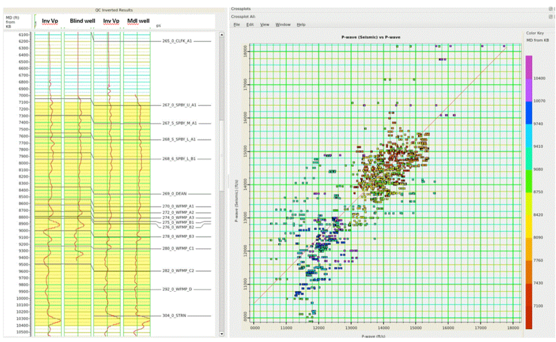

Figure 1c: Correlation of simultaneous prestack inversion with bandpass filtered well logs on the given and blind wells. Correlation coefficient 0.73 at blind well.

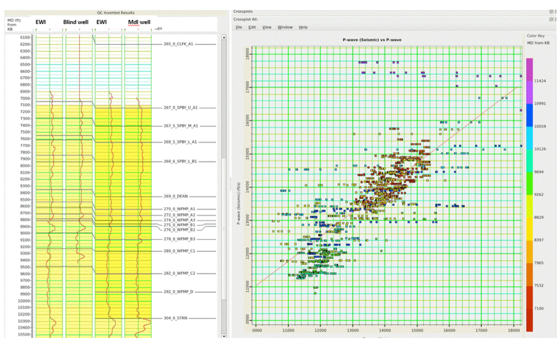

Figure 1d: Correlation of EWI Vp with strict flat gathers with bandpass filtered well logs on the given and blind wells. Correlation coefficient 0.78 at the blind well.

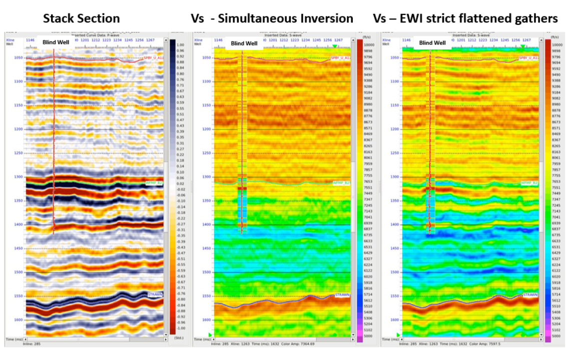

Figure 2a: Shear-wave velocity comparison of simultaneous prestack seismic inversion (center) with EWI on strict flattened gathers (right) passing through the blind well.

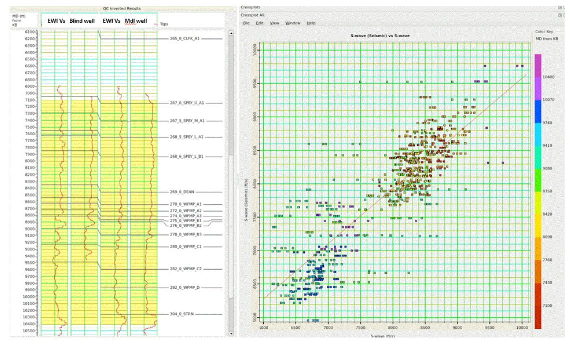

Figure 2b: Correlation of Vs EWI with strict flattened gathers to the input and blind well filtered logs. Correlation coefficient of 0.8 for the blind well.

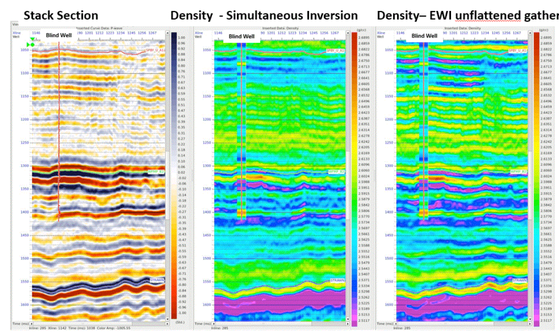

Figure 3a: Bulk density comparison of simultaneous prestack seismic inversion (center) with EWI on non strict flattened gathers (right).

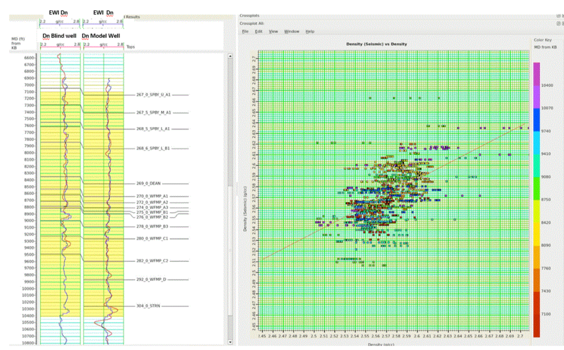

Figure 3b: Comparison of Rho EWI with strict flattened gathers to the input and blind well filtered logs. Correlation coefficient of 0.54 with the blind well.

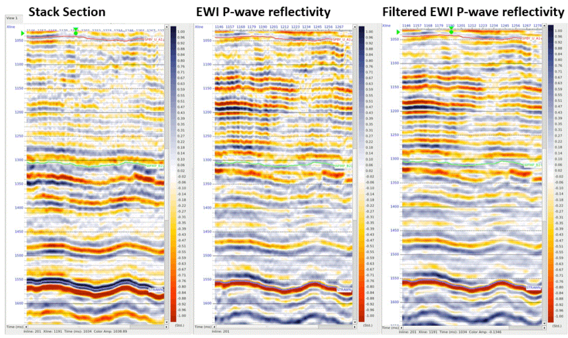

Figure 4:. Comparison of production PSTM stack left and EWI based unfiltered P-wave reflectivity (center) and filtered EWI based P-wave reflectivity (right)